

Supplementary

A multi-analyte responsive chemosensor vanilinyI Schiff base: fluorogenic sensing to Zn(II), Cd(II) and I[†]

Rakesh Purkait, Sunanda Dey and Chittaranjan Sinha*

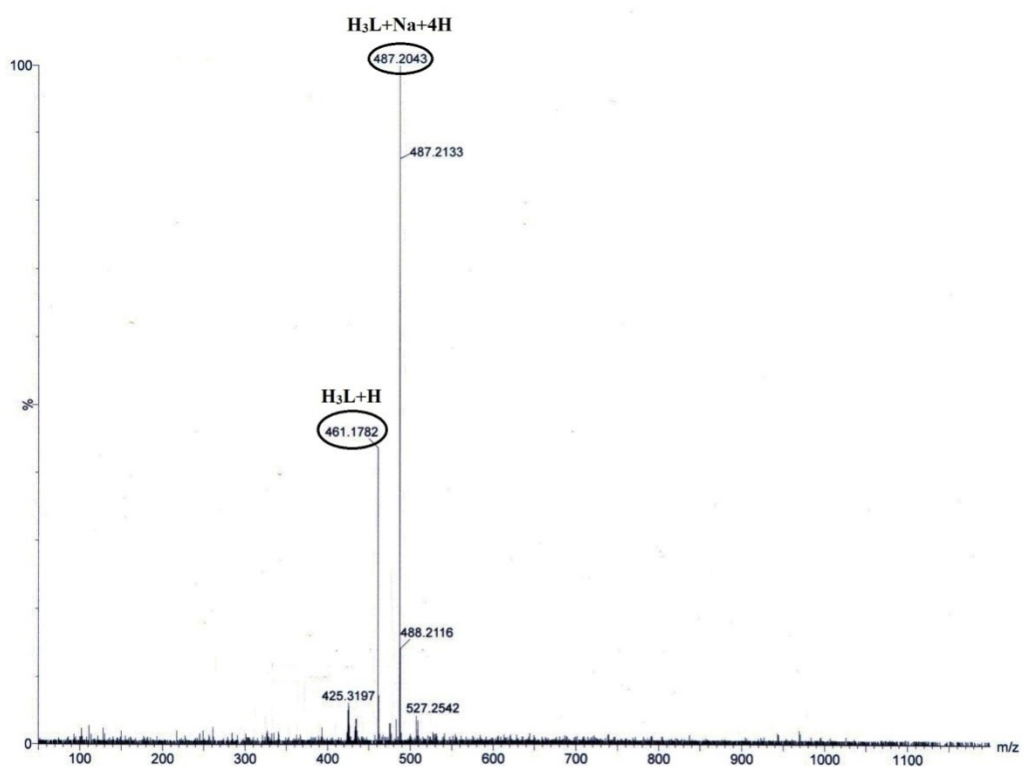


Fig. S1 MS of H₃L

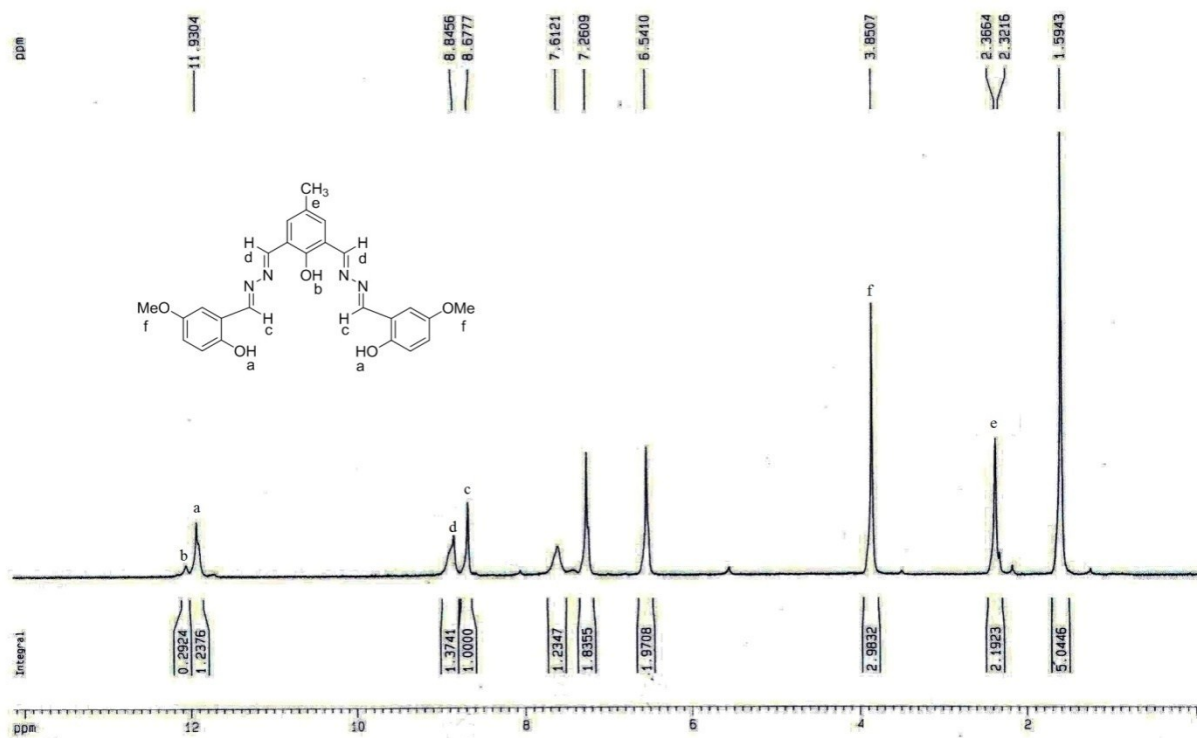


Fig. S2 ¹H NMR of H₃L in CDCl₃

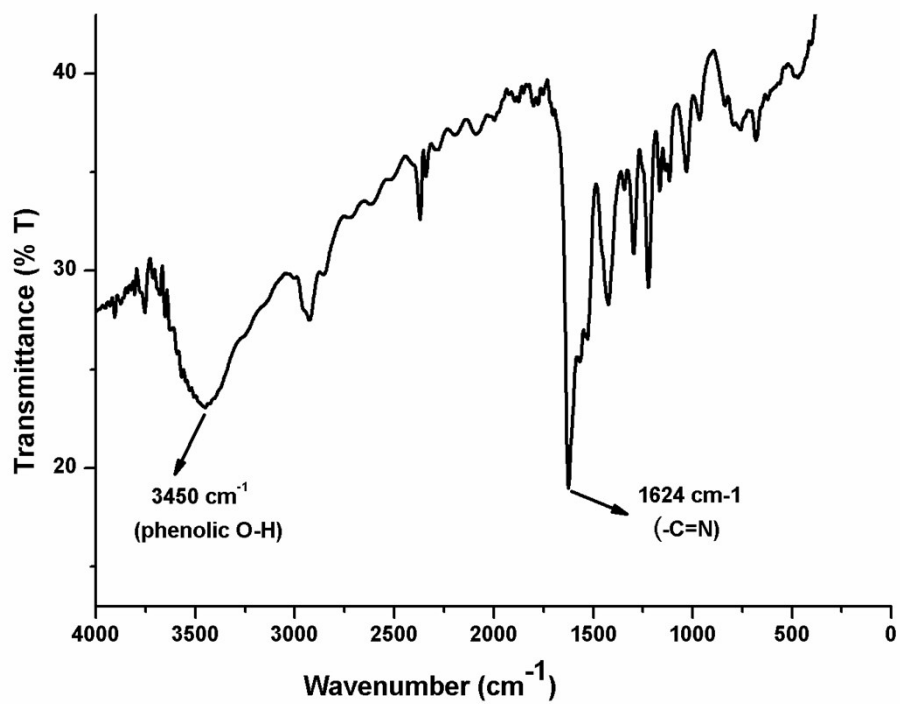


Fig.S3 IR of H₃L

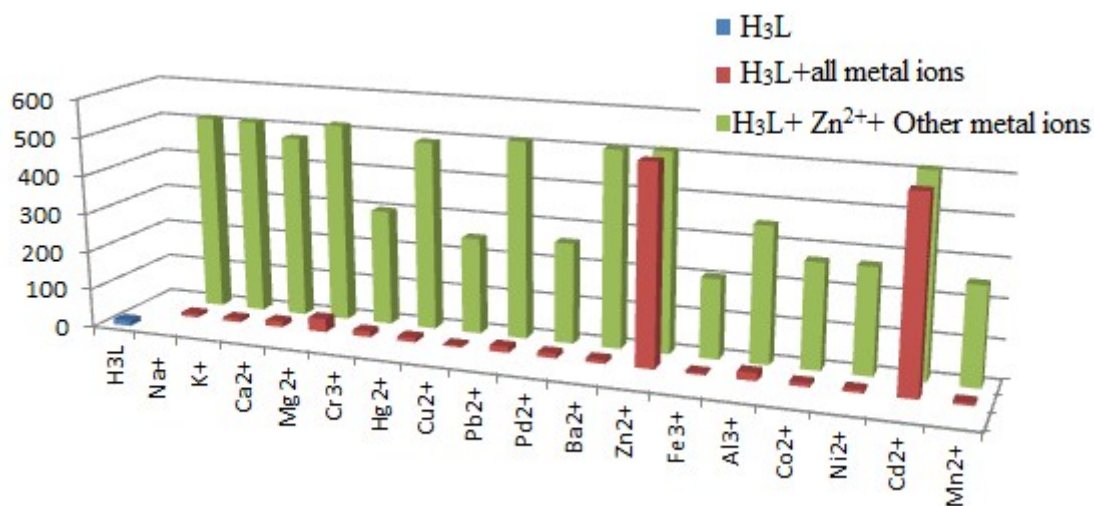


Fig.S4: Interferences study by various metal ions on Zn²⁺ sensitivity

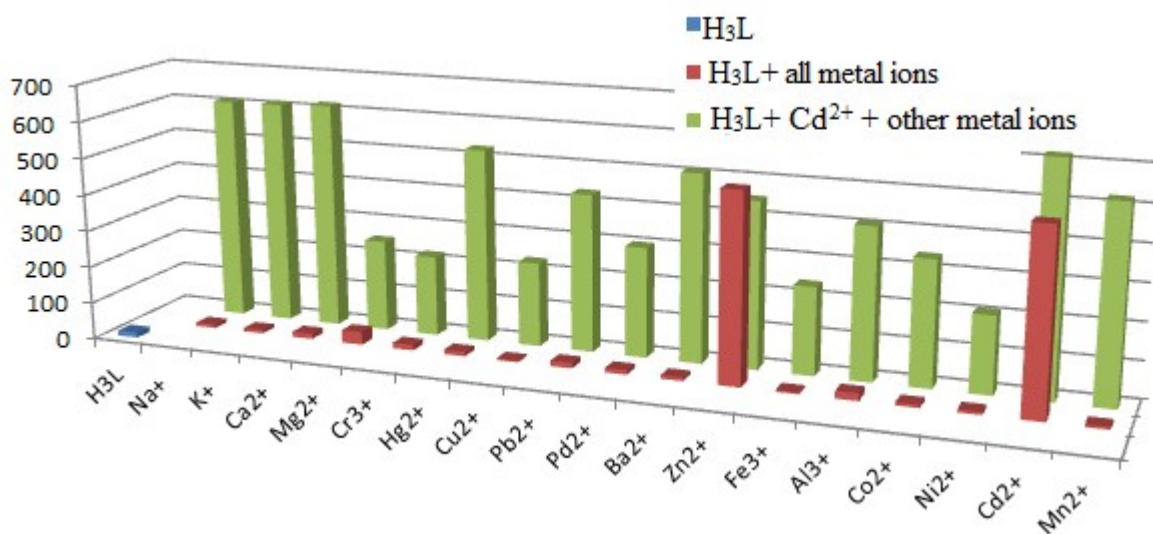


Fig.S5: Interferences study by various metal ions on Cd²⁺ sensitivity

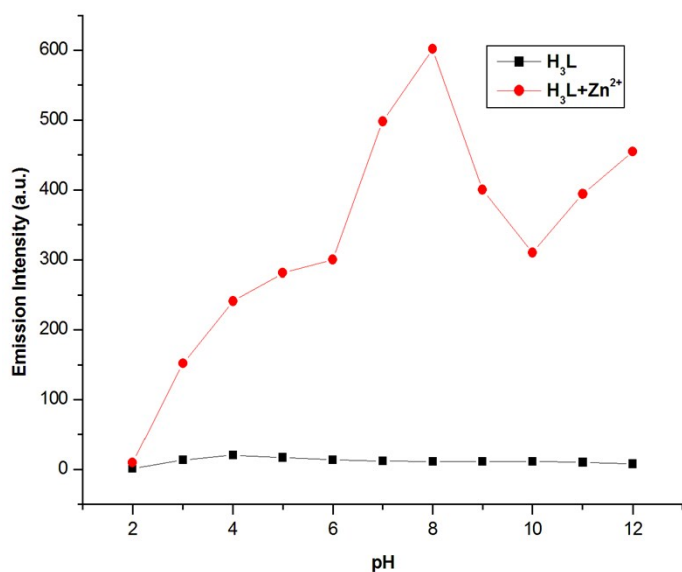


Fig.S6 Effect of pH variation on Zn²⁺ sensitivity

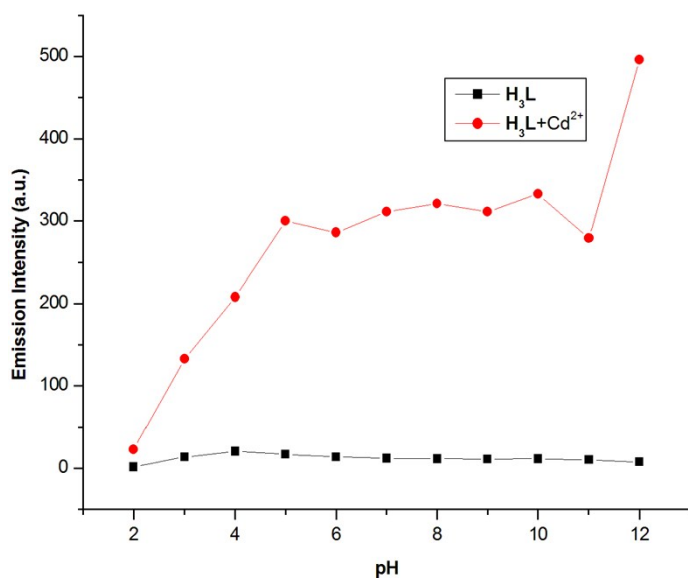


Fig.S7 Effect of pH variation on Cd²⁺ sensitivity

Determination of detection limit:

The detection limit was calculated based on the fluorescence titration. To determine the S/N ratio, the emission intensity of H₃L without any analyte was measured by 10 times. The limit of detection (LOD) of H₃L for Zn²⁺ and Cd²⁺ was determined from the following equation: $LOD = K \times \sigma$ Where $K = 3$ in this case and $\sigma = (Sb_1)/(S)$; Sb_1 is the standard deviation of the blank solution; S is the slope of the calibration curve. For Zn²⁺, From the graph we get slope = 2.478×10^8 , and Sb_1 value is 0.2257(Fig. S8). Thus using the formula we get the LOD =

2.7×10^{-9} M. For Cd^{2+} , From the graph we get slope = 2.478×10^8 , and S_b value is 0.2312 (Fig. S9). Thus using the formula we get the LOD = 6.6×10^{-9} M.

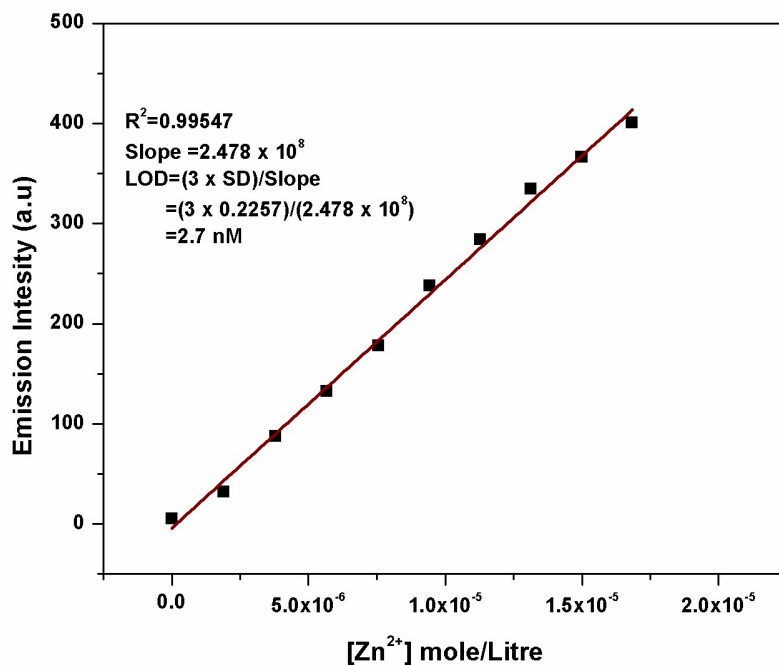


Fig S8 LOD plot for Zn^{2+}

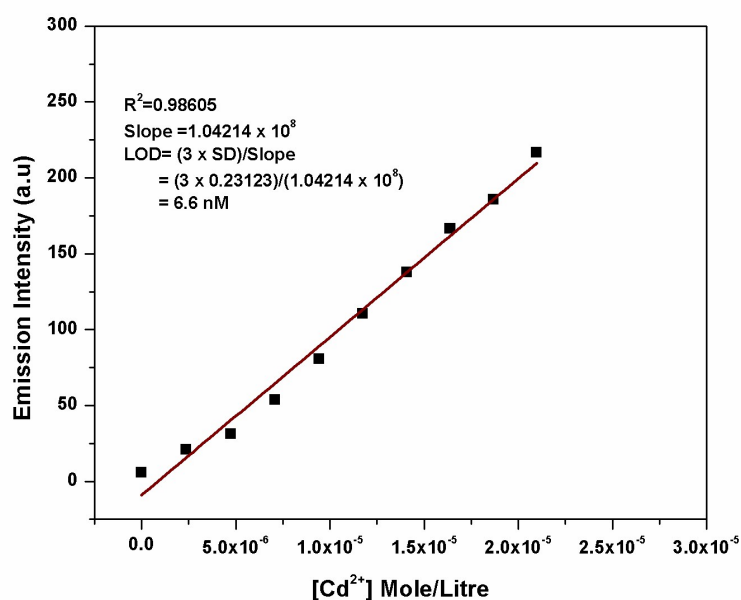
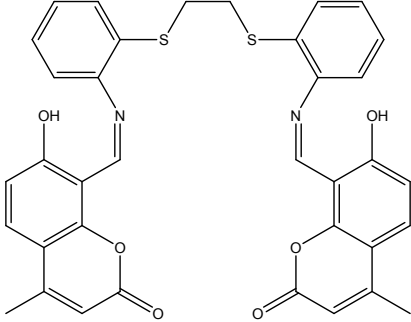
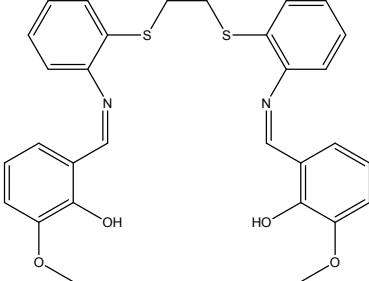
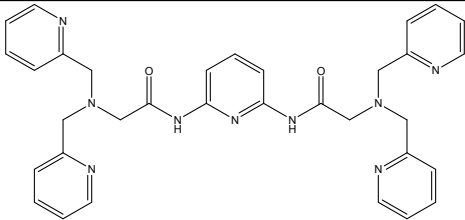
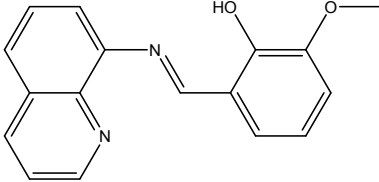
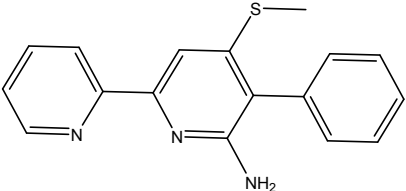
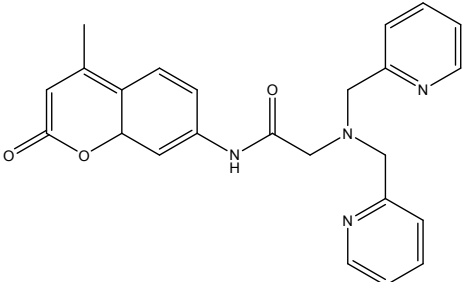
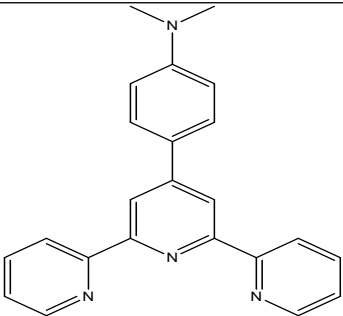
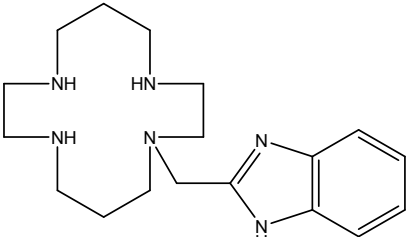
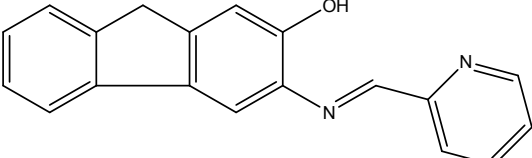
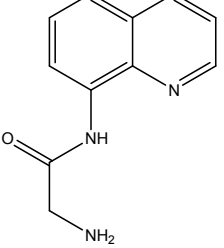
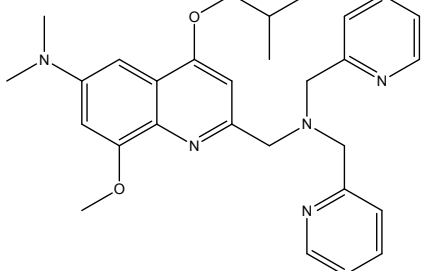
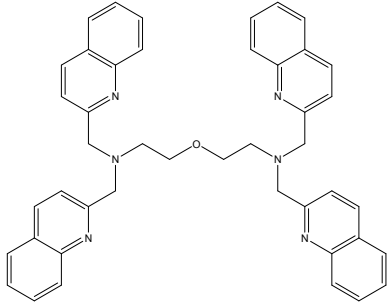
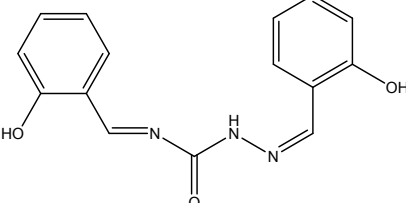
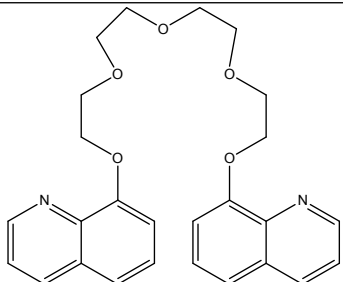
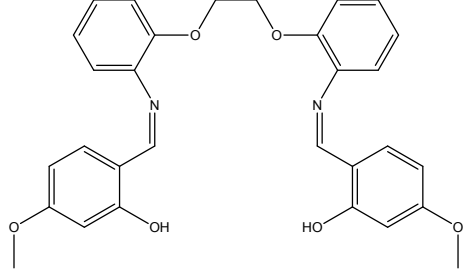
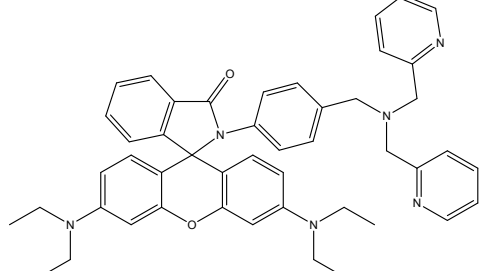


Fig S9 LOD plot for Cd^{2+}

Table S1. Comparison of LOD of similar type fluorogenic probe to Zn^{2+}/Cd^{2+}

Serial No.	Probe	Sensitivity	LOD	Reference
1		Zn^{2+}	6.7×10^{-6} M.	8
2		Zn^{2+}	62×10^{-9} M	39
3		Zn^{2+}	-	45
4		Zn^{2+}	1.3×10^{-7} M	46
5		Zn^{2+}	5×10^{-6} M	47
6		Zn^{2+}, Cd^{2+}	-	48

7		Zn ²⁺ , Cd ²⁺	1.84 × 10 ⁻⁷ M, 1.76 × 10 ⁻⁷ M	49
8		Zn ²⁺ , Cd ²⁺ , Cu ²⁺	-	50
9		Zn ²⁺ , Cd ²⁺	0.61 × 10 ⁻⁶ M, 0.53 × 10 ⁻⁶ M	51
10		Zn ²⁺	1.6 × 10 ⁻⁶ M	52
11		Cd ²⁺	9.6 × 10 ⁻¹² M	53
12		Cd ²⁺	22 × 10 ⁻⁹ M	54
13		Cd ²⁺	5 × 10 ⁻⁴ M	55

14		Cd^{2+}	8.4×10^{-6} M.	56
15		Zn^{2+}	18×10^{-9} M	57
16		Zn^{2+}	-	58

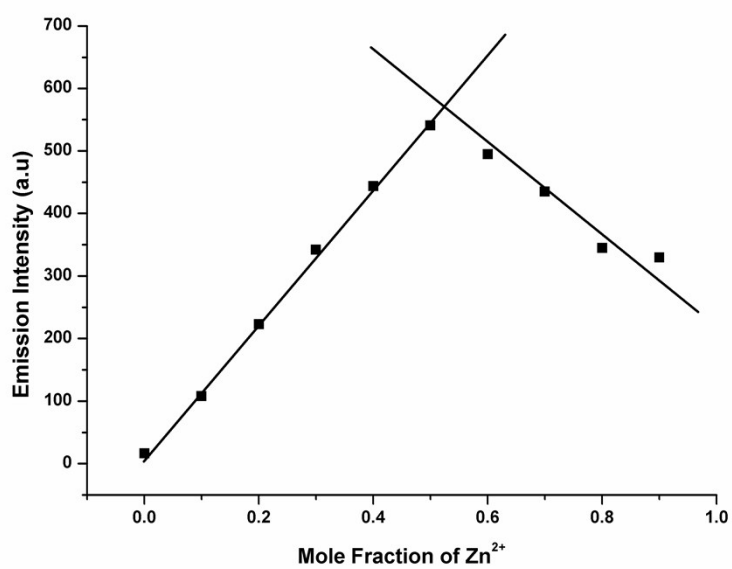


Fig.S10The Job's plot obtained by fluorescence experiment for Zn^{2+}

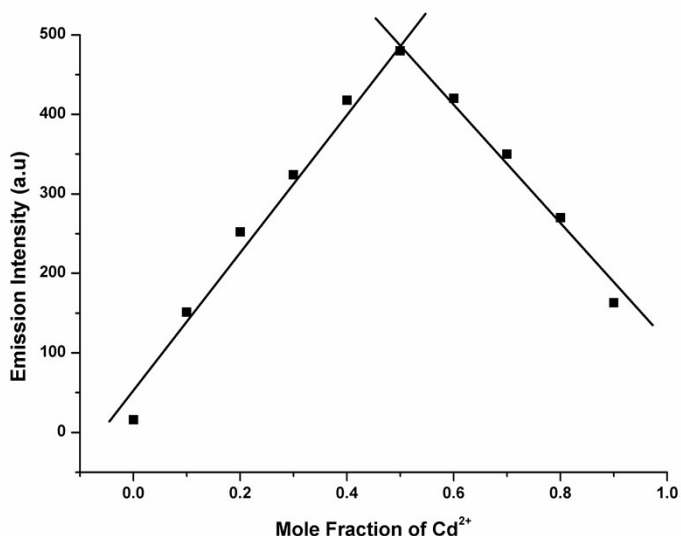


Fig. S11 The Job's plot obtained by fluorescence experiment for Cd²⁺

Determination of binding constant :

The binding constant value of Zn²⁺ and Cd²⁺ with H₃L has been determined from the emission intensity data following the modified Benesi–Hildebrand equation, $1/\Delta F = 1/\Delta F_{\max} + (1/K[C])(1/\Delta F_{\max})$. Here $\Delta F = F - F_{\min}$ and $\Delta F_{\max} = F_{\max} - F_{\min}$, where F_{\min} , F , and F_{\max} are the emission intensities of H₃L considered in the absence of ions, at an intermediate ions concentration, and at a concentration of complete saturation where K is the binding constant and $[C]$ is the anions concentration respectively. In this report we represent F_{\min} as F_0 . From the plot of $(F_{\max} - F_0)/(F - F_0)$ against $[C]^{-1}$ for ions, the value of K has been determined from the slope. The association constant (K_d) as determined by fluorescence titration method for H₃L with Zn²⁺ is found to be $2.7 \times 10^4 \text{ M}^{-1}$ (error < 10%) and for H₃L with Cd²⁺ is found to be $0.96 \times 10^4 \text{ M}^{-1}$ (error < 10%).

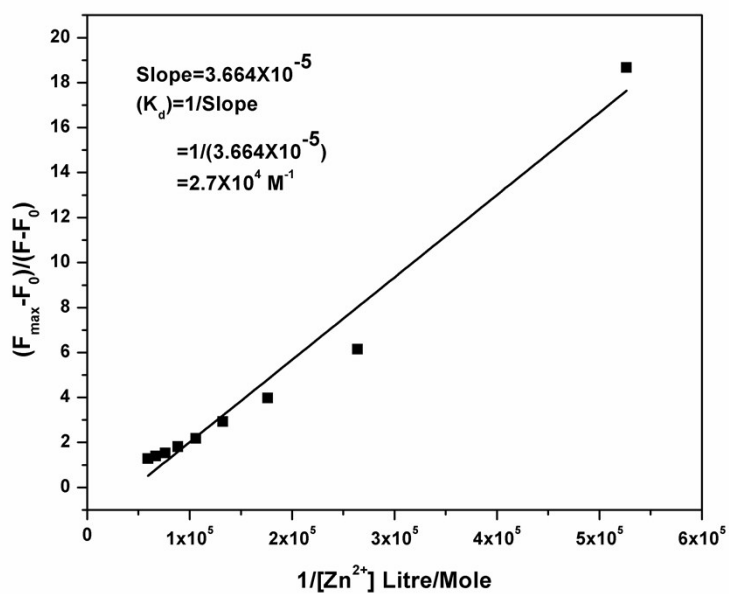


Fig.S12 Benesi–Hildebrand plot for addition of Zn^{2+} with H_3L

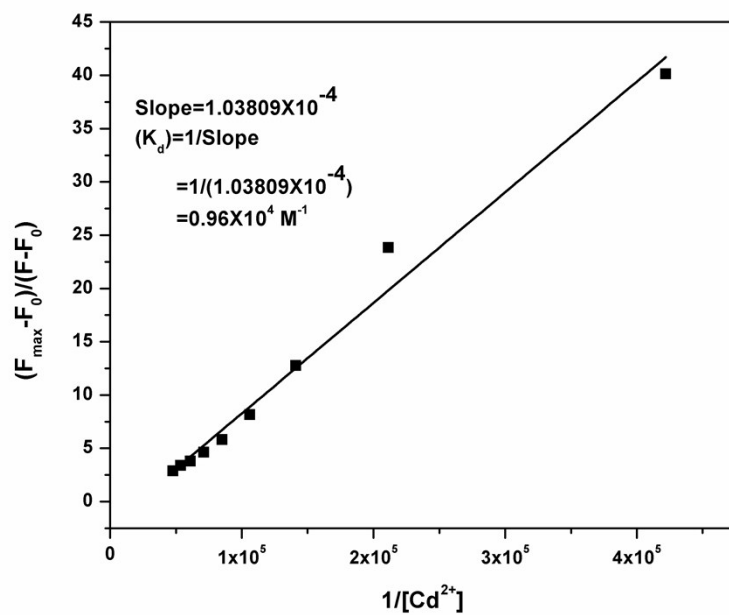


Fig. S13 Benesi–Hildebrand plot for addition of Cd^{2+} with H_3L

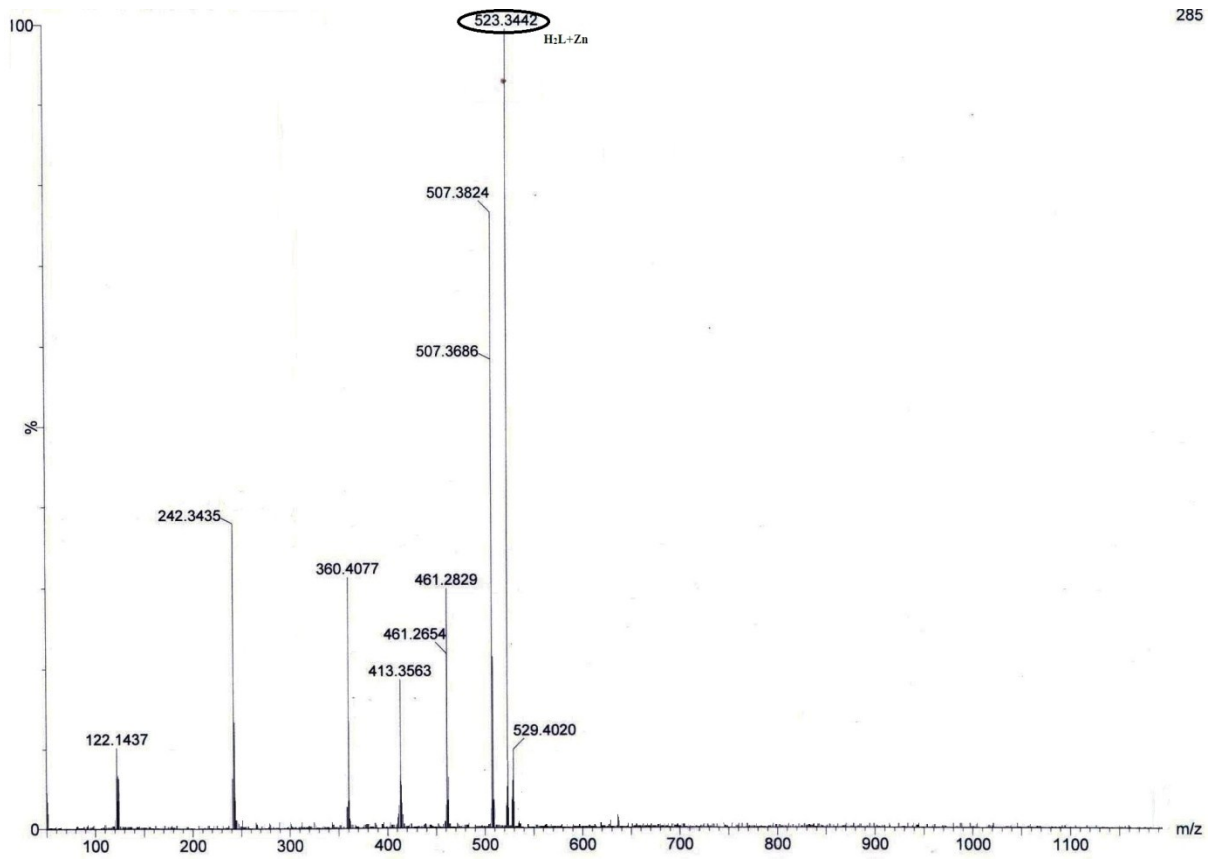


Fig. S14 MS of Zn complex

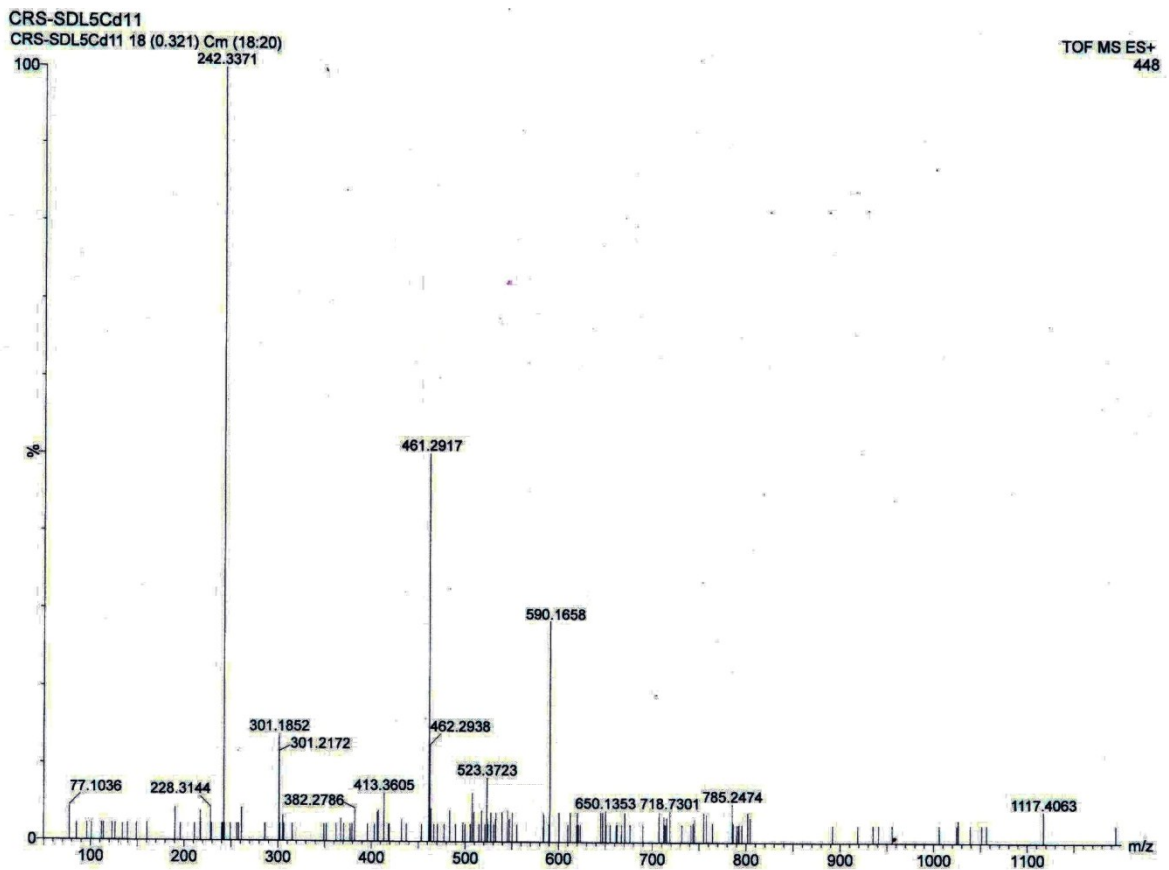


Fig. S15 MS of Cd complex

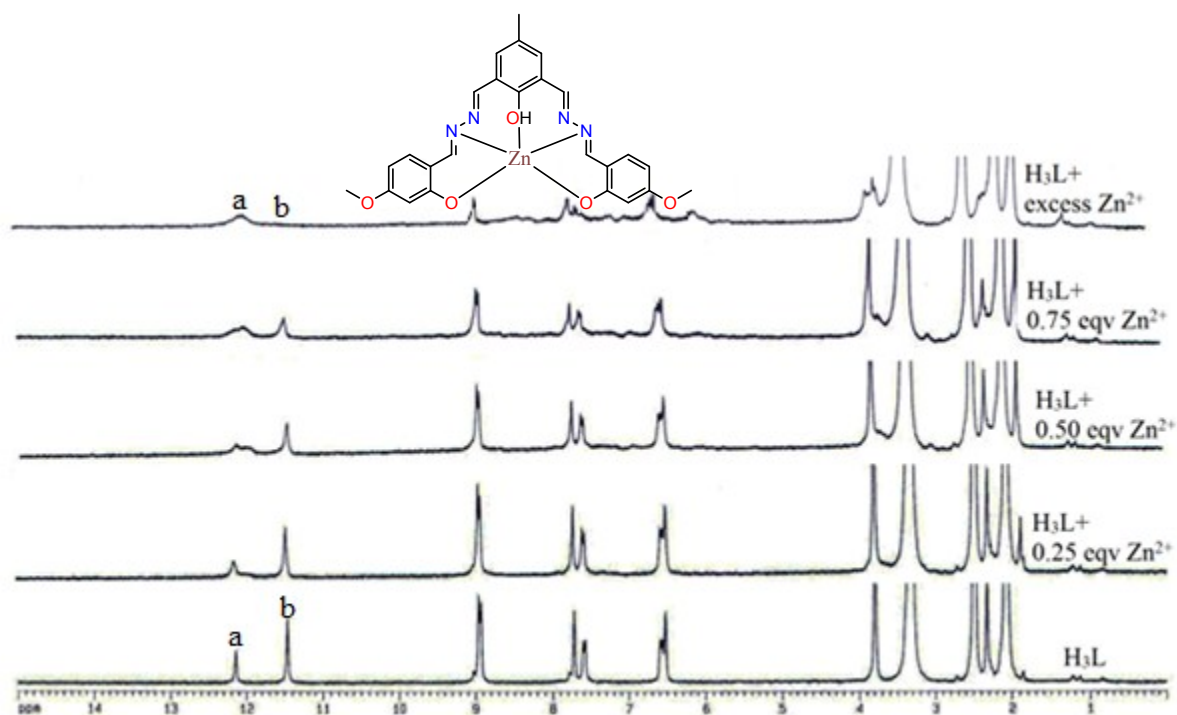


Fig.S16: ¹H NMR titration of H₃L with Zn²⁺ in DMSO-d₆

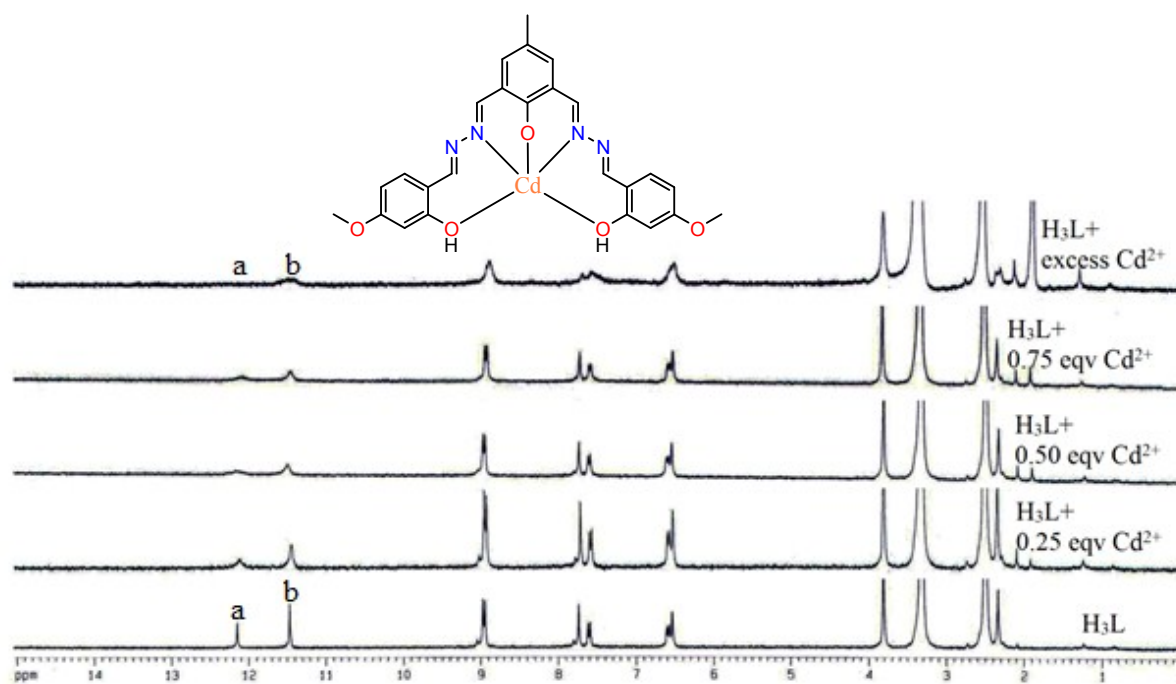


Fig.S17: ¹H NMR titration of H₃L with Cd²⁺ in DMSO-d₆

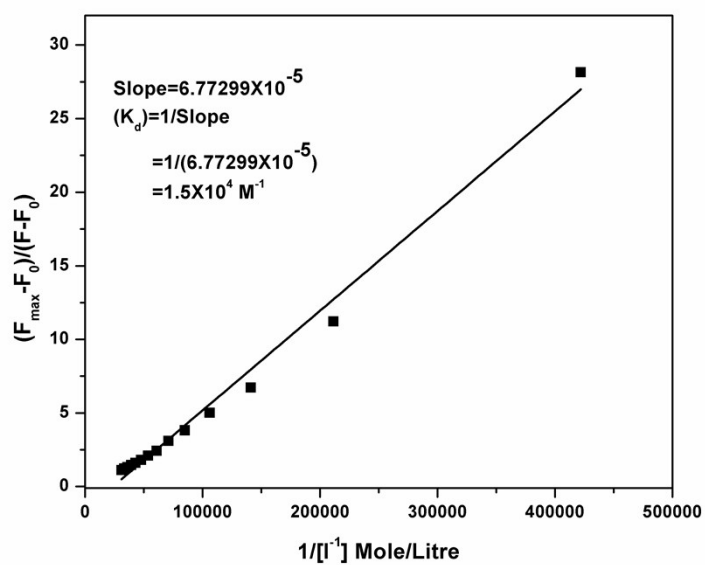


Fig. S18 Fluorimetric titration determines the binding constant for I⁻ (Benesi–Hildebrand plot)



Fig. S19: ESI-MS spectrum of H₃L-I⁻

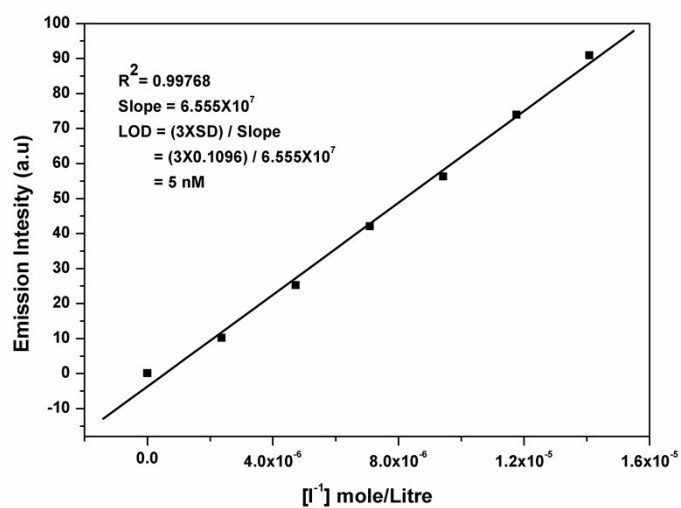
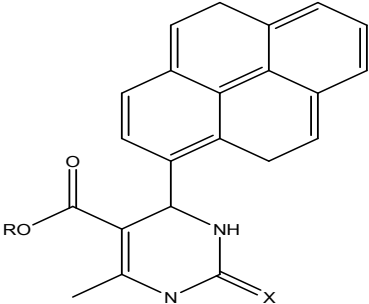
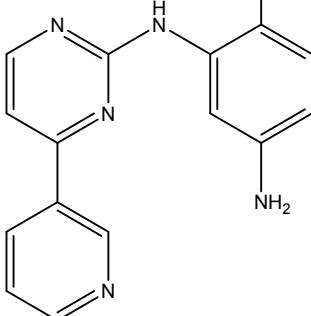
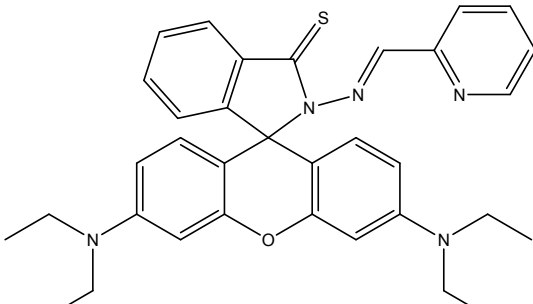
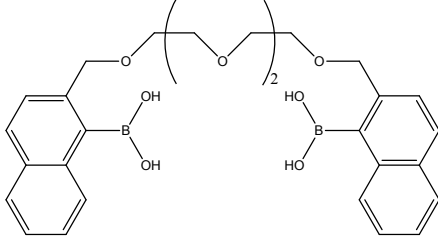
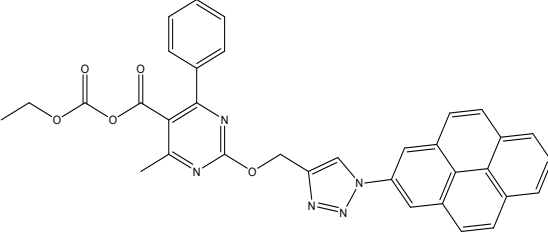


Fig. S20: LOD plot for I⁻

Table S2: Comparison of Iodide (I⁻) sensor efficiency

Serial No.	Probe	LOD	Reference
1		1.2×10^{-6} M	14
2		22.6×10^{-9} M	59

3	<p style="text-align: center;">Hg complex of</p> 	0.2×10^{-9} M	60
4		0.22×10^{-6} M	61
5	<p style="text-align: center;">Hg complex of</p> 	-	62
6		52×10^{-6} M	63
7		0.33×10^{-6} M	64

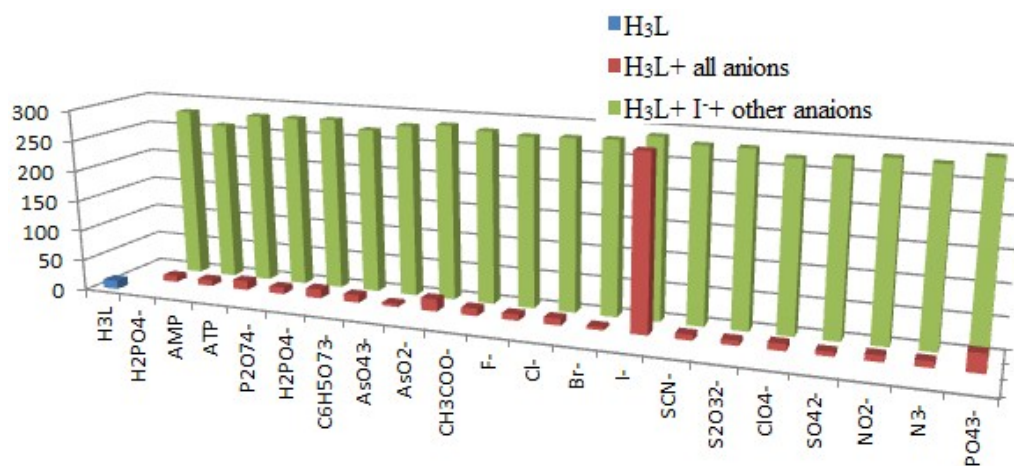


Fig.S21: Interferences study by various metal ions on I⁻ sensitivity

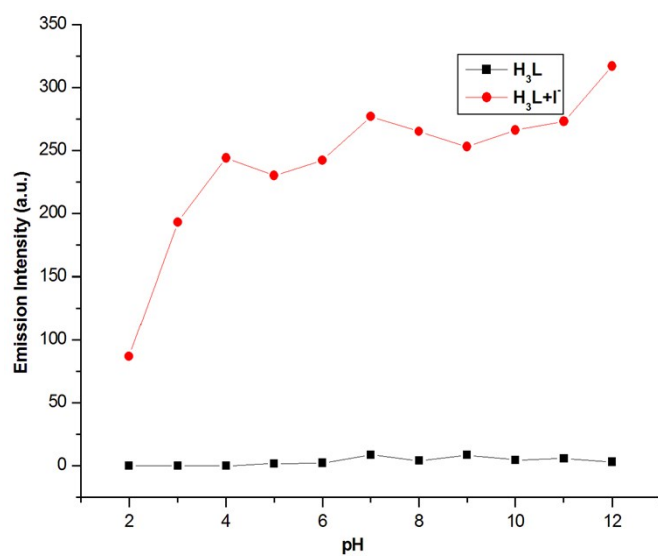


Fig. S22 Effect of pH variation on I⁻ sensitivity

Table S3 optimised structure and bond parameters of H₃L-Zn²⁺

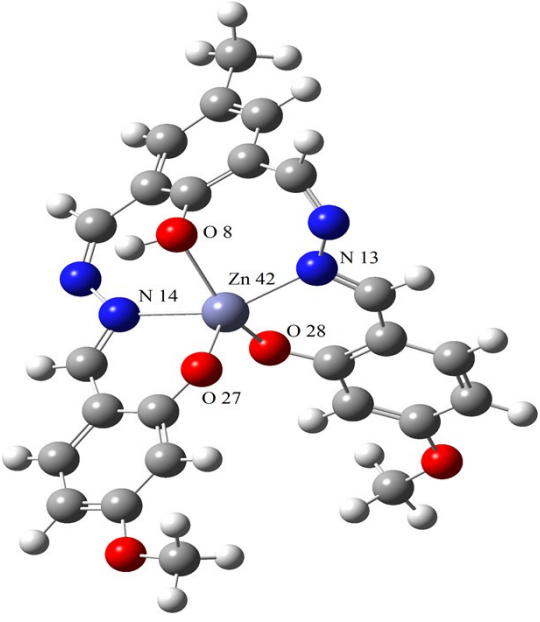
Optimise structure of H ₃ L-Zn ²⁺ complex	Bond Length	Bond angle
	Zn(42) - O(8), 2.22 Å	O(8) - Zn(42) - N(14), 74.20°
	Zn(42) - N(14), 2.22 Å	N(14) - Zn(42) - O(27), 88.41°
	Zn(42) - O(27), 1.96 Å	O(27) - Zn(42) - O(28), 110.39°
	Zn(42) - O(28), 1.97 Å	O(28) - Zn(42) - N(13), 88.98°
	Zn(42) - N(13), 2.13 Å	N(13) - Zn(42) - O(8), 84.12°

Table S4 optimised structure and bond parameters of H₃L-Cd²⁺

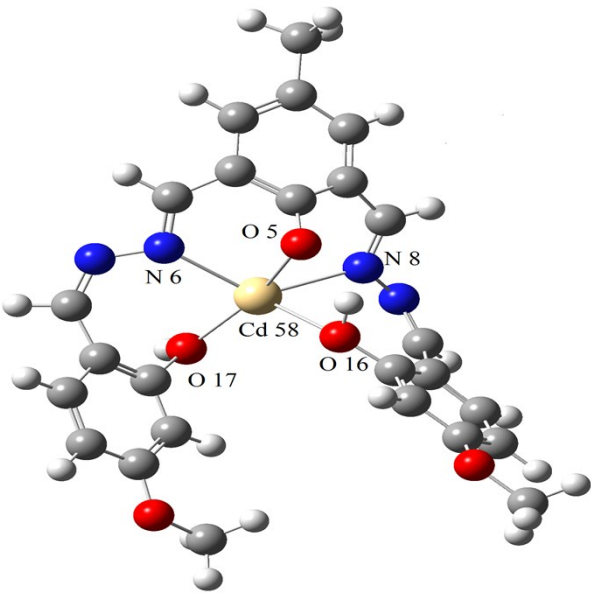
Optimized structure of H ₃ L-Cd ²⁺ complex	Bond Length	Bond angle
	Cd(58) - O(5), 2.22 Å	O(5) - Cd(58) - N(8), 74.4°
	Cd(58) - N(8), 2.41 Å	N(8) - Cd(58) - O(16), 72.55°
	Cd(58) - O(16), 2.29 Å	O(16) - Cd(58) - O(17), 114.79°
	Cd(58) - O(17), 2.23 Å	O(17) - Cd(58) - N(6), 86.45°
	Cd(58) - N(6), 2.36 Å	N(6) - Cd(58) - O(5), 78.14°

Table S5 optimised structure and bond parameters of H₃L-I⁻

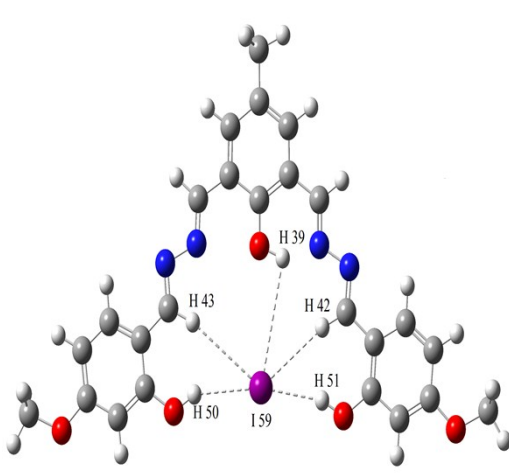
Optimise structure of H ₃ L-I ⁻ complex	Bond Length	Bond angle
	I(59) - H(39), 3.88 Å	H(39) - I(59) - H(42), 42.01°
	I(59) - H(42), 3.10 Å	H(42) - I(59) - H(51), 42.67°
	I(59) - H(51), 2.57 Å	H(51) - I(59) - H(50), 167.58°
	I(59) - H(50), 2.78 Å	H(50) - I(59) - H(43), 37.82°
	I(59) - H(43), 3.41 Å	H(43) - I(59) - H(39), 69.74°

Table S6 comparison of experimental and theoretical transitions

Ligand/Complex	Absorbance wavelength	Excitation energy	transitions
H ₃ L	$\lambda(\text{expt})$ 310 $\lambda(\text{theo})$ 310.62	3.9915 eV	(67%) HOMO-4→LUMO
H ₃ L	$\lambda(\text{expt})$ 337 $\lambda(\text{theo})$ 327.28	3.7883 eV	(87%) HOMO-3→LUMO
H ₃ L	$\lambda(\text{expt})$ 350 $\lambda(\text{theo})$ 349.32	3.5493 eV	(87%) HOMO-1→LUMO+1
H ₃ L	$\lambda(\text{expt})$ 380 $\lambda(\text{theo})$ 384.33	3.2260 eV	(56 %) HOMO-2→LUMO+1
H ₃ L	$\lambda(\text{expt})$ 394 $\lambda(\text{theo})$ 416.75	2.9750 eV	(92%) HOMO→LUMO
H ₃ L-Zn ²⁺	$\lambda(\text{expt})$ 425 $\lambda(\text{theo})$ 422.37	2.9560 eV	(91%) HOMO→LUMO
H ₃ L-Cd ²⁺	$\lambda(\text{expt})$ 480 $\lambda(\text{theo})$ 475.45	2.6077 eV	(89%) HOMO→LUMO
H ₃ L-I ⁻	$\lambda(\text{expt})$ 555 $\lambda(\text{theo})$ 571.94	2.1678 eV	(54%) HOMO→LUMO+1

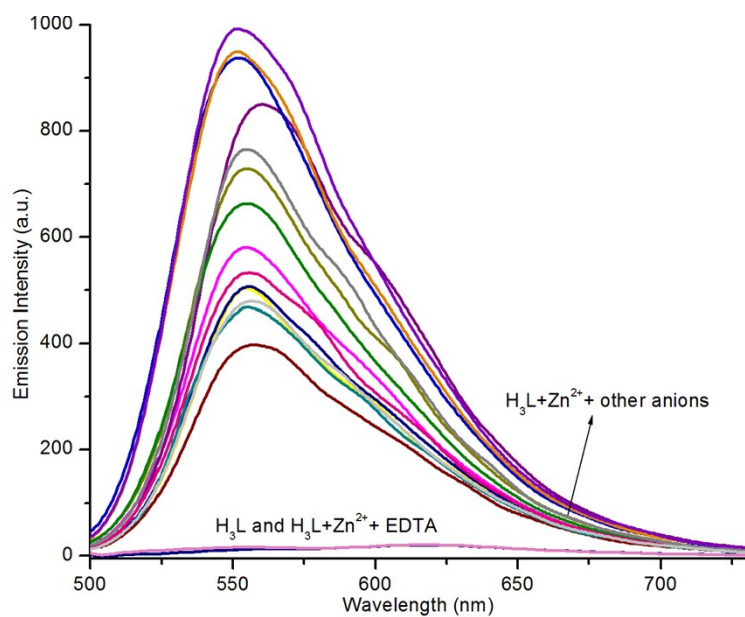


Fig.S23 reversibility with anions of Zn complex

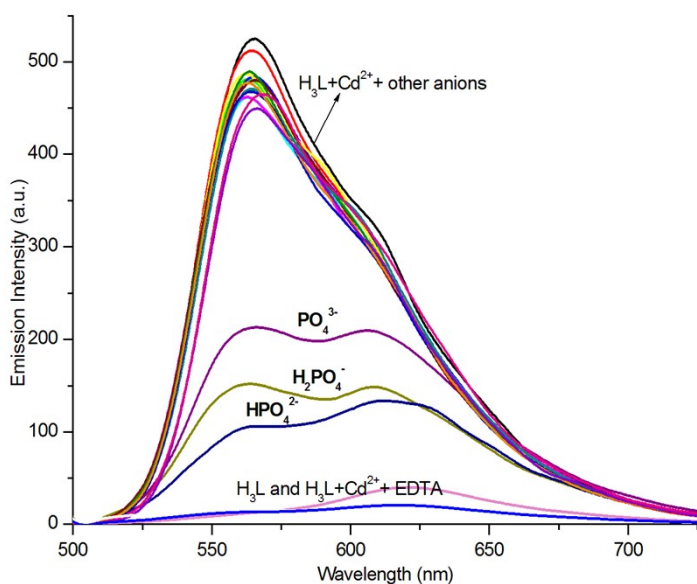


Fig. S24reversibility with anions of Cd complex

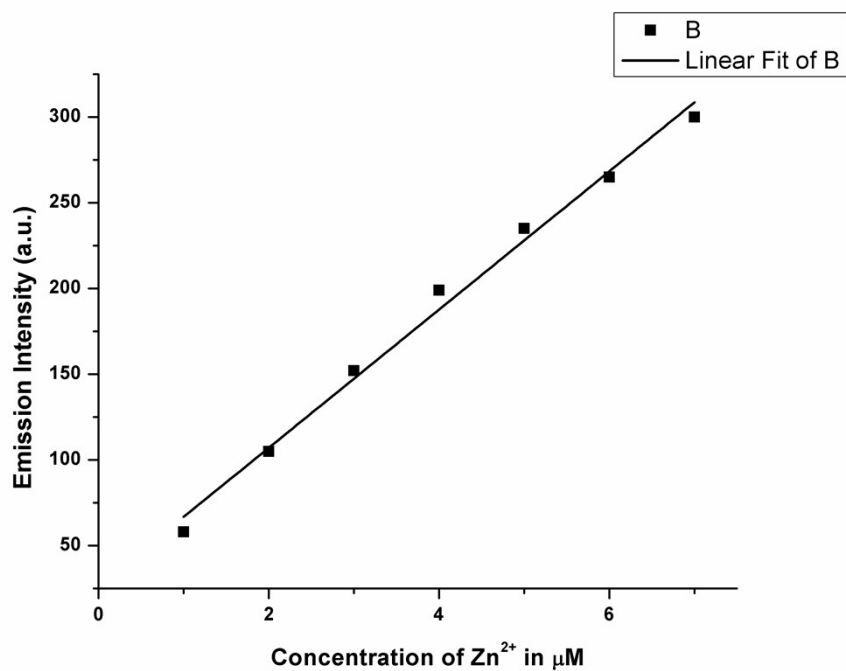


Fig. S25: Calibration plot between emission intensity of the probe H₃L at 545 nm vs Zn²⁺ ion for the quantitative analysis of Zn²⁺ ion in drinking water.

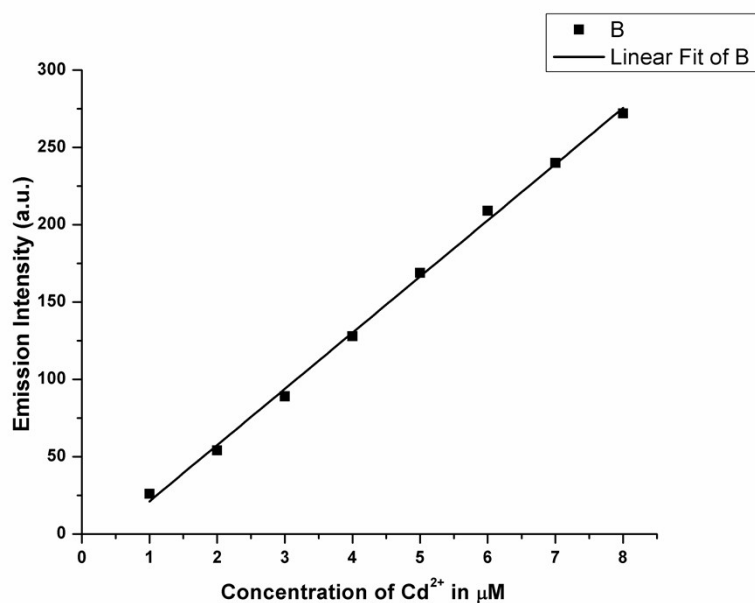


Fig. S26: Calibration plot between emission intensity of the probe H₃L at 560 nm vs Cd²⁺ ion for the quantitative analysis of Cd²⁺ ion in drinking water.